SCIENCE CHINA
Information Sciences

• RESEARCH PAPER •

May 2026, Vol. 69, Iss. 5, 152201:1–152201:15
https://doi.org/10.1007/s11432-025-4644-x

Monotonically-increasing-function-based event-triggered sampling scheme for stabilization of networked nonlinear systems

Xian-Ming ZHANG[1], Qing-Long HAN[1*], Baolin ZHANG[2] & Xiaohua GE[1]

[1]*School of Engineering, Swinburne University of Technology, Melbourne VIC 3122, Australia*
[2]*College of Automation and Electronic Engineering, Qingdao University of Science & Technology, Qingdao 266061, China*

Received 5 March 2025/Revised 7 July 2025/Accepted 9 September 2025/Published online 29 January 2026

Abstract This paper is concerned with event-triggered stabilization of a class of nonlinear networked systems. First, a novel event-triggered sampling scheme is proposed based on a monotonically increasing function in the form of the integral of the error norm between the current state and the latest triggered state. It is proven that this scheme ensures the minimum inter-event time to be strictly greater than zero in an explicit expression. Second, a novel Lyapunov functional tailored for the proposed event-triggered scheme is constructed. By applying the looped functional method, a sampling-interval-dependent stabilization criterion is derived. This criterion provides an algorithm to co-design both control gains and event-triggered parameters for a given threshold. Finally, a practical system comprising two identical pendulums is given to demonstrate the effectiveness of the proposed method.

Keywords event-triggered sampling, networked systems, stabilization, nonlinear systems, looped functional method

Citation Zhang X-M, Han Q-L, Zhang B L, et al. Monotonically-increasing-function-based event-triggered sampling scheme for stabilization of networked nonlinear systems. Sci China Inf Sci, 2026, 69(5): 152201, https://doi.org/10.1007/s11432-025-4644-x

1 Introduction

Over the past two decades, event-triggered control (ETC) has attracted considerable attention in the field of networked control systems. Unlike conventional periodic sampling, ETC samples system signals only when specific events occur or certain predefined conditions are violated, rather than at fixed time intervals. This feature enables ETC to optimize the use of network resources, reduce data transmission and storage requirements, and maintain real-time responsiveness to dynamic system changes. Numerous notable contributions on this topic can be found in [1–12] and the references therein.

Beyond its theoretical advancements, ETC holds significant promise for practical engineering applications, particularly in networked and resource-constrained environments [13–20]. By updating control actions or transmitting data only when necessary, ETC can substantially lower communication and computation demands, making it well suited for wireless sensor networks, industrial automation, and various cyber-physical systems. For example, ETC can help prolong the operational lifetime of battery-powered distributed sensors, mitigate network congestion in smart grids, and enhance the efficiency of remote or embedded controllers. This synergy between theoretical development and practical feasibility underscores ETC as a promising approach for next-generation intelligent and sustainable control architectures.

Recalling the existing results on event-triggered control, an emulation-based approach is often employed [1]. The basic idea is to design a suitable event-triggered scheme for a given controller, ensuring that some certain performance (e.g., stability) of the sampled-data system can be preserved [21–25]. For convenience of presentation, it is assumed that the control input is given as $u(t) = Fx(s_k)$, where F is a known control gain, x the system state, and s_k the latest event instant with $k = \{1, 2, \ldots, \}$. The key challenge is to devise an event-triggering condition to calculate the next event instant s_{k+1}. Let $\ell_k = s_{k+1} - s_k$. A fundamental concern is to ensure that the minimum lower bound ℓ_m of ℓ_k is strictly greater than zero to exclude the occurrence of Zeno behavior [26].

To address this issue, several notable event-triggering conditions have been reported in [1, 22, 24, 25, 27–29]. Initially, static event-triggering conditions are introduced, where an event is triggered when the norm of the system

* Corresponding author (email: qhan@swin.edu.au)

state or error exceeds a predefined fixed threshold. While this approach significantly reduces communication and control updates compared to periodic sampling, it often results in conservative designs due to the difficulty of selecting an optimal threshold. To improve flexibility, adaptive and dynamic event-triggering conditions are developed, offering a larger minimum lower bound ℓ_m compared to static event-triggering conditions. Further advancements lead to integral-based event-triggering conditions, where control updates are determined by accumulated deviations over time rather than instantaneous violations, enhancing robustness.

When designing event-triggering conditions to sample system states, it is crucial to ensure a positive lower bound ℓ_m to prevent Zeno behavior. However, according to the Nyquist-Shannon theorem, it is equally important to ensure the existence of an upper bound ℓ_M of ℓ_k to maintain adequate sampling rates and avoid information loss. Despite this, most of the existing event-triggering conditions focus solely on ensuring ℓ_m while ignoring ℓ_M.

To illustrate this, we consider three representative classes of event-triggering conditions reported in the literature:

$$\begin{aligned}
&e^{\mathrm{T}}(t)\mathscr{Q}e(t)-\sigma_0 x^{\mathrm{T}}(t_k)\mathscr{Q}x(t_k)>0,\\
&\int_{s_k}^{t} e^{\mathrm{T}}(r)\mathscr{Q}e(r)\mathrm{d}r-\int_{s_k}^{t}\sigma_0 x^{\mathrm{T}}(r)\mathscr{Q}x(r)\mathrm{d}r>0,\\
&\int_{s_k}^{t} e^{\mathrm{T}}(r)\mathrm{d}r\mathscr{Q}\int_{s_k}^{t} e(r)\mathrm{d}r-\sigma_0 x^{\mathrm{T}}(s_k)\mathscr{Q}x(s_k)>0,
\end{aligned}$$

where $e(t)=x(t)-x(s_k)$, $\mathscr{Q}>0$ is a weighted matrix and $\sigma_0>0$ is a threshold. Under these conditions, it is proven that a positive ℓ_m can be guaranteed for systems without disturbances. However, ensuring a finite upper bound ℓ_M remains challenging. As a result, most stability analyses based on these conditions are independent of ℓ_M, leading to conservative designs. Therefore, in event-triggered sampling, it is essential to design an event-triggering condition that considers both ℓ_m and ℓ_M, which is the key motivation for this study.

This paper investigates the problem of event-triggered stabilization of a class of nonlinear networked systems. A novel event-triggering condition is introduced as

$$\mathscr{T}(t)=\int_{s_k}^{t} e^{\mathrm{T}}(r)\mathscr{Q}e(r)\mathrm{d}r-\sigma_0 x^{\mathrm{T}}(s_k)\mathscr{Q}x(s_k)>0,$$

leading to a novel event-triggered sampling scheme (ESS). A key feature of $\mathscr{T}(t)$ is its monotonic increase with respect to time t. It is proven that this scheme not only prevents Zeno behavior but also provides an explicit expression for the minimum inter-event time. Comparative analysis demonstrates that this scheme is more suitable than some existing ones, particularly when the signal varies slowly. Moreover, the monotonicity of $\mathscr{T}(t)$ ensures that the sampling intervals are upper bounded under the proposed ESS, in line with the principle of Nyquist-Shannon theorem. Next, a looped functional tailored for the ESS is constructed. By employing the looped functional method [30], a sampling-interval-dependent criterion is derived to ensure that the closed-loop system under the ESS is asymptotically stable. Moreover, the obtained criterion facilitates the co-design of both a suitable control gain and a weighted matrix in the ESS. Finally, a practical system is given to demonstrate the effectiveness of the proposed method.

Notations. Throughout this paper, col$\{\cdots\}$ means a column-block vector and diag$\{\cdots\}$ a diagonal matrix. He$\{A\}=A+A^{\mathrm{T}}$. $\mathbb{R}$ is a set of real number and $\mathbb{Z}_{\geqslant 0}$ ($\mathbb{Z}_{>0}$) a set of non-negative (positive) integers. $\lambda_{\min}(Q)$ ($\lambda_{\max}(Q)$) stands for the minimum (maximum) eigenvalue of Q. The symbol '$\star$' denotes a symmetric term in a symmetric matrix.

2 Problem statement

Consider a networked system with a nonlinear physical plant described by

$$\begin{cases}\dot{x}(t)=Ax(t)+Bu(t)+Cg(t,x(t)),\\ x(s_0)=\phi_0,\end{cases}\tag{1}$$

where $x\in\mathbb{R}^n$ and $u\in\mathbb{R}^m$ are the system state and system input, respectively; and ϕ_0 is the system initial state. The system matrices $A,C\in\mathbb{R}^{n\times n}$ and $B\in\mathbb{R}^{n\times m}$ are constant matrices. ϕ_0 is the system initial state at $t=s_0$. The nonlinear function $g(t,x)$ may be piecewise-continuous, mapping from $\mathbb{R}^{n+1}$ to $\mathbb{R}^n$, in both arguments t and

x. This nonlinear function can be regarded as system disturbances or uncertainties. All one knows about it is that it belongs to the following set $\mathcal{S}_\rho$:

$$\mathcal{S}_\rho = \left\{ g(t,x) : \mathbb{R}^{n+1} \to \mathbb{R}^n \;\middle|\; g^{\mathrm{T}}(t,x)g(t,x) \leqslant \rho^2 x^{\mathrm{T}}\Lambda^{\mathrm{T}}\Lambda x \right\},$$

where $\rho > 0$ is a scalar and Λ is a known compatible real matrix. Clearly, $g(t,0) = 0$ if $g \in \mathcal{S}_\rho$. If $g(t,x)$ is a sector-nonlinear function, then the system (1) is called a Lur'e system. Thus, the system described by (1) includes the Lur'e system as its special case.

The system (1) is fully investigated in [31]. Its aim is to design a suitable controller $u(t) = Fx(t)$ as well as maximize the parameter ρ such that the resulting closed-loop system is asymptotically stable for $\forall g(t,x) \in \mathcal{S}_\rho$. Under network environments, this problem is addressed in [32, 33] to investigate how the network-induced delays and packet loss affect the allowable upper bound of ρ. In this paper, we focus on the stabilization problem of the system (1) under an event-triggered sampling scheme.

Suppose that the system state is available for state feedback control. The control signals are computed on the basis of sampled state. Let the sampling instants be $\{s_1, s_2, \ldots, s_k \ldots\}$ with $\lim_{k\to\infty} s_k = \infty$. Then the control signal is given by

$$u(t) = Fx(s_k),\ s_k \leqslant t < s_{k+1}, \tag{2}$$

where F is the control gain. Under the controller (2), the resulting closed-loop system associated with (1) reads as, for $k \in \mathbb{Z}_{\geqslant 0}$

$$\dot{x}(t) = Ax(t) + BFx(s_k) + Cg(t,x(t)),\ s_k \leqslant t < s_{k+1}. \tag{3}$$

In what follows, we introduce a novel ESS to calculate the sampling instants $\{s_1, s_2, \ldots, s_k, \ldots\}$, which is given by

$$\text{ESS1}: \quad \begin{cases} s_k = s_0, & k = 0, \\ s_{k+1} = \inf\left\{ t > s_k \mid \mathscr{T}(t) > 0 \right\}, & k \geqslant 1, \end{cases} \tag{4}$$

where

$$\mathscr{T}(t) \triangleq \int_{s_k}^{t} e^{\mathrm{T}}(\theta)\mathscr{Q}e(\theta)\mathrm{d}\theta - \sigma_0 x^{\mathrm{T}}(s_k)\mathscr{Q}x(s_k), \tag{5}$$

$$e(t) = x(t) - x(s_k) \tag{6}$$

with $\mathscr{Q} > 0$ being a weighted matrix and $\sigma_0 > 0$ a threshold.

The ESS1 involves an integral term $\int_{s_k}^{t} e^{\mathrm{T}}(\theta)\mathscr{Q}e(\theta)\mathrm{d}\theta$, which can be rewritten as $\int_{s_k}^{t} \|\mathscr{Q}^{\frac{1}{2}}e(\theta)\|^2\mathrm{d}\theta$. Thus, the integral term is the integral of the square of the weighted error norm $\|\mathscr{Q}^{\frac{1}{2}}e(\theta)\|$, which is monotonically increasing with respect to time. The main idea behind the ESS1 is that it triggers an event once the accumulation of $\|\mathscr{Q}^{\frac{1}{2}}e(\theta)\|^2$ reaches or gets across over a fixed value of $\sigma_0 x^{\mathrm{T}}(s_k)\mathscr{Q}x(s_k)$. It is a more reasonable way to trigger an event [34]. However, several questions arise:

(i) Under the ESS1, is the Zeno behavior excluded?

(ii) What are the advantages of the ESS1 compared to some existing ones?

(iii) How is the event-triggered condition $\mathscr{T}(t) > 0$ integrated in the stability analysis of the closed-loop system (3)?

This paper provides some solutions to the questions above. The problems to be addressed in this paper can be stated as follows.

• Insightful analysis of the ESS1. Prove theoretically that the Zeno behavior does not occur when ESS1 works, and provide evidence to show the advantages of the ESS1.

• Stability analysis. With the ESS1, for a given control gain F, seek a stability criterion for (3) to ensure the parameter ρ as large as possible.

• Control design. For a given threshold σ_0, co-design a proper control gain F and a proper weighted matrix $\mathscr{Q}$ such that the closed-loop system (3) is asymptotically stable for $\forall g \in \mathcal{S}_\rho$ with ρ being as large as possible.

To end this section, we introduce Lemma 1.

Lemma 1 ([35]). Let R_1 and R_2 be two symmetric positive definite real matrices. For the state vector $x(t)$ and the sampling instants s_k and s_{k+1}, the following inequalities hold:

$$-\int_{s_k}^{t}\dot{x}^{\mathrm{T}}(v)R_1\dot{x}(v)\mathrm{d}v \leqslant -\frac{1}{t-s_k}\chi_1^{\mathrm{T}}(t)\Gamma_0^{\mathrm{T}}\mathcal{R}_1\Gamma_0\chi_1(t),$$
$$-\int_{t}^{s_{k+1}}\dot{x}^{\mathrm{T}}(v)R_2\dot{x}(v)\mathrm{d}v \leqslant -\frac{1}{s_{k+1}-t}\chi_2^{\mathrm{T}}(t)\Gamma_0^{\mathrm{T}}\mathcal{R}_2\Gamma_0\chi_2(t),$$

where $\mathcal{R}_i=\mathrm{diag}\{R_i,3R_i,5R_i\}$ $(i=1,2)$

$$\Gamma_0=\begin{bmatrix} I & -I & 0 & 0\\ I & I & -2I & 0\\ I & -I & -6I & 12I\end{bmatrix},$$
$$\chi_1(t)=\mathrm{col}\left\{x(t),x(s_k),\int_{s_k}^{t}\frac{x(v)}{t-s_k}\mathrm{d}v,\int_{s_k}^{t}\frac{(t-v)x(v)}{(t-s_k)^2}\mathrm{d}v\right\},$$
$$\chi_2(t)=\mathrm{col}\left\{x(s_{k+1}),x(t),\int_{t}^{s_{k+1}}\frac{x(v)}{s_{k+1}-t}\mathrm{d}v,\int_{t}^{s_{k+1}}\frac{(s_{k+1}-v)x(v)}{(s_{k+1}-t)^2}\mathrm{d}v\right\}.$$

Lemma 2 ([36]). Let $\phi(t)\in\mathbb{W}[a,b]$ satisfy $\phi(a)=0$. Then for $n\times n$ real matrix $R>0$ the following inequality holds:

$$\int_a^b\dot{\phi}^{\mathrm{T}}(s)R\dot{\phi}(s)\mathrm{d}s\geqslant\frac{\pi^2}{4(b-a)^2}\int_a^b\phi^{\mathrm{T}}(s)R\phi(s)\mathrm{d}s. \tag{7}$$

3 Insightful analysis of the ESS1

In this section, we make some insightful analyses to show the advantages of the ESS1.

3.1 Exclusion of Zeno behavior

For an event-triggered sampling scheme, the Zeno behavior means an infinite number of events over a finite time period. Thus, to avoid the Zeno behavior, the inter-event time between two consecutive events should be strictly greater than zero. For the ESS1, we have the following conclusion.

Theorem 1. Let s_k be the latest sampling instant for the system (3). The next sampling time s_{k+1} is calculated by the ESS1. Then the time interval $s_{k+1}-s_k$ between two sampling instants s_k and s_{k+1} satisfies

$$s_{k+1}-s_k>\sqrt[3]{\frac{\sigma_0\pi^2x^{\mathrm{T}}(s_k)\mathscr{Q}x(s_k)}{\mathscr{N}^2(s_k)}}, \tag{8}$$

where

$$\mathscr{N}(s_k)=2(\|\mathscr{Q}^{\frac{1}{2}}A\|+\rho\|\mathscr{Q}^{\frac{1}{2}}C\|\|\Lambda\|)X_{s_k}+2\|\mathscr{Q}^{\frac{1}{2}}BF\|\|x(s_k)\|, \tag{9a}$$
$$X_{s_k}=\max_{t\in[s_k,s_{k+1})}\|x(t)\|. \tag{9b}$$

Proof. Suppose $x(s_k)\neq 0$ for $k=1,2,\ldots$ (otherwise, finite-time stabilization is achieved). From the ESS1 (4), one has $\mathscr{T}(s_{k+1})>0$. That is

$$\int_{s_k}^{s_{k+1}}e^{\mathrm{T}}(t)\mathscr{Q}e(t)\mathrm{d}t>\sigma_0x^{\mathrm{T}}(s_k)\mathscr{Q}x(s_k). \tag{10}$$

Note that $e(t)=x(t)-x(s_k)$. Clearly, $e(t)|_{t=s_k}=0$ and $\dot{e}(t)=\dot{x}(t)$. Employing the Wirtinger inequality (Lemma 2), one has

$$\int_{s_k}^{s_{k+1}}\dot{x}^{\mathrm{T}}(t)\mathscr{Q}\dot{x}(t)\mathrm{d}t\geqslant\frac{\pi^2}{4(s_{k+1}-s_k)^2}\int_{s_k}^{s_{k+1}}e^{\mathrm{T}}(t)\mathscr{Q}e(t)\mathrm{d}t. \tag{11}$$

Following from (10) and (11) yields

$$(s_{k+1}-s_k)^2 > \frac{\sigma_0\pi^2 x^{\mathrm{T}}(s_k)\mathscr{Q}x(s_k)}{4\int_{s_k}^{s_{k+1}}\dot{x}^{\mathrm{T}}(t)\mathscr{Q}\dot{x}(t)\mathrm{d}t}. \tag{12}$$

Note that from (3), $\dot{x}(t)=Ax(t)+BFx(s_k)+Cg(t,x(t))$. Then

$$\begin{aligned}\|\mathscr{Q}^{\frac{1}{2}}\dot{x}(t)\| &\leqslant \|\mathscr{Q}^{\frac{1}{2}}Ax(t)\|+\|\mathscr{Q}^{\frac{1}{2}}BFx(s_k)\|+\|\mathscr{Q}^{\frac{1}{2}}Cg(t,x(t))\|\\ &\leqslant \|\mathscr{Q}^{\frac{1}{2}}Ax(t)\|+\|\mathscr{Q}^{\frac{1}{2}}BFx(s_k)\|+\rho\|\mathscr{Q}^{\frac{1}{2}}C\|\|\Lambda x(t)\|\\ &\leqslant (\|\mathscr{Q}^{\frac{1}{2}}A\|+\rho\|\mathscr{Q}^{\frac{1}{2}}C\|\|\Lambda\|)X_{s_k}+\|\mathscr{Q}^{\frac{1}{2}}BF\|\|x(s_k)\|.\end{aligned} \tag{13}$$

Then it follows from (12) and (13) that

$$(s_{k+1}-s_k)^3 > \frac{\sigma_0\pi^2 x^{\mathrm{T}}(s_k)\mathscr{Q}x(s_k)}{\mathscr{N}^2(s_k)}, \tag{14}$$

where $\mathscr{N}(s_k)$ is given in (9a), which leads to (8).

Next, we prove by contradiction that Zeno behavior is excluded. Suppose that Zeno behavior occurs. Then for arbitrarily small positive number $\epsilon>0$, there exists a sufficiently large integer k^* such that

$$s_{k+1}-s_k<\epsilon,\ \forall k>k^*. \tag{15}$$

In this situation, from (9b), one has $X_{s_k}=\max_{t\in[s_k,s_{k+1})}\|x(t)\|\leqslant\max_{t\in[s_k,s_k+\epsilon)}\|x(t)\|\to\|x(s_k)\|$ due to arbitrarily small ϵ. Thus, from (14)

$$\begin{aligned}(s_{k+1}-s_k)^3 &> \frac{\sigma_0\pi^2\lambda_{\min}(\mathscr{Q})\|x(s_k)\|^2}{4(\|\mathscr{Q}^{\frac{1}{2}}A\|+\rho\|\mathscr{Q}^{\frac{1}{2}}C\|\|\Lambda\|+\|\mathscr{Q}^{\frac{1}{2}}BF\|)^2\|x(s_k)\|^2}\\ &= \epsilon_0 \triangleq \frac{\sigma_0\pi^2\lambda_{\min}(\mathscr{Q})}{4(\|\mathscr{Q}^{\frac{1}{2}}A\|+\rho\|\mathscr{Q}^{\frac{1}{2}}C\|\|\Lambda\|+\|\mathscr{Q}^{\frac{1}{2}}BF\|)^2},\end{aligned} \tag{16}$$

which is in contradiction with (15) if choosing $\epsilon=\sqrt[3]{\epsilon_0}>0$. This completes the proof.

Remark 1. Theorem 1 provides an explicit expression for the lower bound of the sampling interval $s_{k+1}-s_k$, which depends on the system state at s_k, system matrices A,B,F and the event-triggering parameters $\sigma_0,\mathscr{Q}$. Moreover, with this expression, it is proven that Zeno behavior is excluded under the ESS1.

3.2 Comparison with some existing event-triggered schemes

In this section, we make comparisons with some existing event-triggered schemes. Event-triggered schemes usually involve the following event-triggering conditions [1, 22, 25]:

$$\mathscr{T}_1(t)=e^{\mathrm{T}}(t)\mathscr{Q}e(t)-\sigma_0x^{\mathrm{T}}(t_k)\mathscr{Q}x(t_k)>0, \tag{17}$$

$$\mathscr{T}_2(t)=\int_{s_k}^{t}e^{\mathrm{T}}(r)\mathscr{Q}e(r)\mathrm{d}r-\int_{s_k}^{t}\sigma_0x^{\mathrm{T}}(r)\mathscr{Q}x(r)\mathrm{d}r>0, \tag{18}$$

$$\mathscr{T}_3(t)=\int_{s_k}^{t}e^{\mathrm{T}}(r)\mathrm{d}r\mathscr{Q}\int_{s_k}^{t}e(r)\mathrm{d}r-\sigma_0x^{\mathrm{T}}(s_k)\mathscr{Q}x(s_k)>0, \tag{19}$$

and the so-called dynamic event-triggering condition [29]

$$\mathscr{T}_4(t)=\eta(t)+\theta[\sigma_0x^{\mathrm{T}}(t)\mathscr{Q}x(t)-e^{\mathrm{T}}(t)\mathscr{Q}e(t)]\geqslant 0, \tag{20a}$$

$$\dot{\eta}(t)=-\beta(\eta(t))+\sigma_0x^{\mathrm{T}}(t)\mathscr{Q}x(t)-e^{\mathrm{T}}(t)\mathscr{Q}e(t), \tag{20b}$$

where $\beta(\cdot)$ is a locally continuous $\mathcal{K}_\infty$-class function and θ is a positive real number.

We now compare $\mathscr{T}_i(t)$ $(i=1,2,3,4)$ with $\mathscr{T}(t)$ in (4) from the following aspects.

First, an explicit expression for the lower bound of the inter-event time can be derived based on $\mathscr{T}(t)$. However, when considering $\mathscr{T}_1(t)$ and $\mathscr{T}_2(t)$, the lower bound of the inter-event time is typically implied by a certain scalar differential equation, see, e.g., [1, 22]. In [25], it seems that the event-triggered scheme with $\mathscr{T}_3(t)>0$ also provides

an explicit expression for the inter-event time, but this expression depends heavily on the estimation of Taylor expansion.

Second, $\mathscr{T}(t)$ is a monotonically increasing function while $\mathscr{T}_i(t)$ $(i=1,2,3,4)$ may not. To show that, one has

$$\begin{aligned}
\dot{\mathscr{T}}_1(t) &= 2e^{\mathrm{T}}(t)\mathscr{Q}\dot{e}(t),\\
\dot{\mathscr{T}}_2(t) &= e^{\mathrm{T}}(t)\mathscr{Q}e(t)-\sigma_0 x^{\mathrm{T}}(t)\mathscr{D}x(t),\\
\dot{\mathscr{T}}_3(t) &= 2e^{\mathrm{T}}(t)\mathscr{Q}\int_{s_k}^{t}e(\theta)\mathrm{d}\theta,\\
\dot{\mathscr{T}}_4(t) &= -\beta(\eta(t))+\sigma_0 x^{\mathrm{T}}(t)\mathscr{Q}x(t)-e^{\mathrm{T}}(t)\mathscr{Q}e(t)\\
&\quad+\theta\left[2\sigma_0 x^{\mathrm{T}}(t)\mathscr{D}\dot{x}(t)-2e^{\mathrm{T}}(t)\mathscr{D}\dot{e}(t)\right].
\end{aligned}$$

From above, it is clear that determining the sign of $\dot{\mathscr{T}}_i(t)$ $(i=1,2,3,4)$ at any time $t\in[s_k,s_{k+1})$ is not straightforward. Specifically, for $\dot{\mathscr{T}}_4(t)$, it seems that one could select a sufficiently large $\mathcal{K}_\infty$-class function $\beta(\cdot)$ to ensure $\dot{\mathscr{T}}_4(t)<0$ for $\forall t\in[s_k,s_{k+1})$. However, this choice of $\beta(\cdot)$ may not be permissible due to that $\eta(t)$ can be interpreted as a filtered value of $\sigma_0 x^{\mathrm{T}}(t)\mathscr{Q}x(t)-e^{\mathrm{T}}(t)\mathscr{Q}e(t)$ [29].

Now, we turn to $\mathscr{T}(t)$ in ESS1 (4). Taking its derivative yields $\dot{\mathscr{T}}(t)=e^{\mathrm{T}}(t)\mathscr{D}e(t)\geqslant 0$ due to $\mathscr{D}>0$, which means that $\mathscr{T}(t)$ is monotonically increasing for $t\in[s_k,s_{k+1})$.

Compared with the $\mathscr{T}_i(t)$-based ESSs $(i=1,2,3,4)$, the monotone increment property of $\mathscr{T}(t)$ provides several inherent advantages for the ESS1 (4).

- Since $\mathscr{T}_i(t)$ $(i=1,2,3,4)$ are non-monotonic functions, $\mathscr{T}_i(t)$-based ESSs may remain inactive when the signal variations (or errors, i.e., $e(t)$) are not large enough to trigger the next event. Nevertheless, ESS1 performs effectively in this scenario. As long as the error $e(t)$ is nonzero, the accumulation of $e^{\mathrm{T}}(t)\mathscr{D}e(t)$ contributes to the value of $\sigma_0 x^{\mathrm{T}}(s_k)\mathscr{D}x(s_k)$, definitely leading to a new event trigger.
- The monotone increment property of $\mathscr{T}(t)$ prevents the ESS1 from exhibiting Zeno behavior. Zeno behavior implies that time t becomes stuck at a certain point. However, provided $e(t)\neq 0$, the monotonic increase of $\mathscr{T}(t)$ ensures that time t progresses forward such that $\mathscr{T}(t)>0$, effectively eliminating the possibility of Zeno behavior.
- The monotone increment property of $\mathscr{T}(t)$ ensures that the sampling intervals $s_{k+1}-s_k$ under ESS1 are upper-bounded if $e(t)\neq 0$, aligning with the principle of the Nyquist-Shannon theorem. In fact, $\mathscr{T}(t)\leqslant 0$ for $\forall t\in[s_k,s_{k+1})$. By the integral mean-value theorem, there exists an $s_k^*\in(s_k,s_{k+1})$ such that

$$(s_{k+1}-s_k)e^{\mathrm{T}}(s_k^*)\mathscr{D}e(s_k^*)=\int_{s_k}^{s_{k+1}}e^{\mathrm{T}}(r)\mathscr{D}e(r)\mathrm{d}r\leqslant\sigma_0 x^{\mathrm{T}}(s_k)\mathscr{D}x(s_k),$$

leading to

$$s_{k+1}-s_k\leqslant\frac{\sigma_0 x^{\mathrm{T}}(s_k)\mathscr{D}x(s_k)}{e^{\mathrm{T}}(s_k^*)\mathscr{D}e(s_k^*)}.\tag{21}$$

However, $\mathscr{T}_i(t)$-based ESSs do not guarantee an upper bound on the sampling intervals $s_{k+1}-s_k$. This explains why most of the results in event-triggered control do not take into account the upper bound of sampling intervals.

Third, specifically, we compare ESS1 with the $\mathscr{T}_4(t)$-based ESS. At first glance, ESS1 may seem to be a special case of the $\mathscr{T}_4(t)$-based ESS when choosing $\eta(t)=\int_{t_k}^{t}e^{\mathrm{T}}(r)\mathscr{D}e(r)\mathrm{d}r$ and setting $\beta(\cdot)=0$. However, it is not true.

- On one hand, as noted in [29], setting $\beta(\cdot)=0$ is not allowed since $\beta(\cdot)$ is a $\mathcal{K}$-class function.
- On the other hand, even if we hypothetically set $\beta(\cdot)=0$, taking the derivative of $\eta(t)$ gives $\dot{\eta}(t)=e^{\mathrm{T}}(t)\mathscr{D}e(t)$. In this case, the corresponding event-triggered condition reads as

$$\tilde{\mathscr{T}}_4(t)=\int_{t_k}^{t}e^{\mathrm{T}}(r)\mathscr{D}e(r)\mathrm{d}r+\theta e^{\mathrm{T}}(t)\mathscr{D}e(t)\leqslant 0.\tag{22}$$

It is clear that the inequality (22) holds only if $e(t)\equiv 0$ for $\forall t\geqslant t_k$ due to $\mathscr{D}>0$. As a result, no event will be triggered under condition (22), making the ESS ineffective.

4 Stability analysis

In this section, we utilize the looped functional method to analyze the stability of the closed-loop system (3). We introduce a novel approach for integrating the event-triggered scheme ESS1 into the analysis of system stability.

To proceed, we introduce some vectors as

$$\begin{aligned}
&\theta_1(t)=\int_{s_k}^{t}\frac{x(v)}{t-s_k}\mathrm{d}v,\ \theta_2(t)=\int_{t}^{s_{k+1}}\frac{x(v)}{s_{k+1}-t}\mathrm{d}v,\\
&\theta_3(t)=(t-s_k)\theta_1(t),\ \theta_4(t)=(s_{k+1}-t)\theta_2(t),\\
&\theta_5(t)=\int_{s_k}^{t}\frac{(t-v)x(v)}{(t-s_k)^2}\mathrm{d}v,\ \theta_6(t)=\int_{t}^{s_{k+1}}\frac{(s_{k+1}-v)x(v)}{(s_{k+1}-t)^2}\mathrm{d}v,\\
&\theta_7(t)=(t-s_k)\theta_5(t),\ \theta_8(t)=(s_{k+1}-t)\theta_6(t),\\
&\varsigma_1(t)=\mathrm{col}\{x(t),x(s_k),x(s_{k+1}),\theta_3(t),\theta_4(t),\theta_7(t),\theta_8(t)\},\\
&\varsigma_2(t)=\mathrm{col}\{e(t),\theta_3(t),\theta_7(t)\},\ e(t)=x(t)-x(s_k),\\
&\varsigma_3(t)=\mathrm{col}\{\varpi(t),\theta_4(t),\theta_8(t)\},\ \varpi(t)=x(s_{k+1})-x(t),\\
&\xi(t)=\mathrm{col}\{\dot{x}(t),\varsigma_1(t),\theta_1(t),\theta_2(t),\theta_5(t),\theta_6(t)\}.
\end{aligned}\tag{23}$$

Choose a Lyapunov functional

$$V(t)=x^{\mathrm{T}}(t)Px(t)+\mathcal{V}_1(t)+\mathcal{V}_2(t)+\mathcal{V}_3(t)+\mathcal{V}_4(t),\tag{24}$$

where

$$\begin{aligned}
\mathcal{V}_1(t)&=2\begin{bmatrix}(s_{k+1}-t)\varsigma_2(t)\\(t-s_k)\varsigma_3(t)\end{bmatrix}^{\mathrm{T}}S_1\varsigma_1(t)+2\varsigma_2^{\mathrm{T}}(t)S_2\varsigma_3(t),\\
\mathcal{V}_2(t)&=(t-s_k)(s_{k+1}-t)\begin{bmatrix}x(s_k)\\x(s_{k+1})\end{bmatrix}^{\mathrm{T}}S_3\begin{bmatrix}x(s_k)\\x(s_{k+1})\end{bmatrix},\\
\mathcal{V}_3(t)&=(s_{k+1}-t)\int_{s_k}^{t}\dot{x}^{\mathrm{T}}(v)R_1\dot{x}(v)\mathrm{d}v-(t-s_k)\int_{t}^{s_{k+1}}\dot{x}^{\mathrm{T}}(v)R_2\dot{x}(v)\mathrm{d}v,\\
\mathcal{V}_4(t)&=-(s_{k+1}-t)\int_{s_k}^{t}e^{\mathrm{T}}(v)\mathscr{Q}e(v)\mathrm{d}v.
\end{aligned}\tag{25}$$

Remark 2. It is not difficult to verify that $\mathcal{V}_j(s_k)=\mathcal{V}(s_{k+1})=0$ $(j=1,\ldots,4)$. Thus, $\mathcal{V}_j(t)$'s are looped functionals. It should be pointed out that $\mathcal{V}_4(t)$ is inspired from the event-triggering function $\mathscr{T}(t)$ in (5) in the ESS1. Therefore, we call $V(t)$ an ESS-dependent Lyapunov functional.

For convenience, we set $\ell_k=s_{k+1}-s_k$, indicating the time interval between two consecutive sampling instants. From the insightful analysis of the ESS1 in the previous section, it is reasonable to suppose that there exist two positive numbers ℓ_m and ℓ_M such that $\ell_m\leqslant\ell_k\leqslant\ell_M$ for $k\in\mathbb{Z}_{\geqslant 0}$.

Now we establish and state the following result.

Proposition 1. For given scalars ρ,ℓ_m,ℓ_M with $\rho\geqslant 0$ and $\ell_M\geqslant\ell_m>0$, a threshold $\sigma_0>0$ and a certain control gain F, the system (3) is asymptotically stable for $\forall g(t,x)\in\mathcal{S}_\rho$ if there exist real matrices $P>0,R_1>0,R_2>0,\mathscr{Q}>0$, real matrices $S_1,S_2,S_3,M_1,M_2,L_1,L_2,X$, and a scalar variable $\lambda>0$ such that, for $\ell_k\in\{\ell_m,\ell_M\}$

$$\Upsilon_1:=\begin{bmatrix}\Omega_0+\ell_k\Omega_1 & XC & \lambda\rho e_2^{\mathrm{T}}\Lambda^{\mathrm{T}} & \ell_kM_2^{\mathrm{T}}\\ \star & -\lambda I & 0 & 0\\ \star & \star & -\lambda I & 0\\ \star & \star & \star & -\ell_k\mathcal{R}_2\end{bmatrix}<0,\tag{26}$$

$$\Upsilon_2:=\begin{bmatrix}\Omega_0+\ell_k\Omega_2 & XC & \lambda\rho e_2^{\mathrm{T}}\Lambda^{\mathrm{T}} & \ell_kM_1^{\mathrm{T}}\\ \star & -\lambda I & 0 & 0\\ \star & \star & -\lambda I & 0\\ \star & \star & \star & -\ell_k\mathcal{R}_1\end{bmatrix}<0,\tag{27}$$

where e_i $(i=1,2,\ldots,12)$ are row-block vectors with the ith entry being an identity matrix and the others zero matrices, and

$$\Omega_0=\mathrm{He}\big\{e_2^{\mathrm{T}}Pe_1+\wp_3^{\mathrm{T}}S_2\wp_6+\wp_4^{\mathrm{T}}S_2\wp_5+(\wp_5^{\mathrm{T}}\mathcal{I}_2^{\mathrm{T}}-\wp_3^{\mathrm{T}}\mathcal{I}_1^{\mathrm{T}})S_1\wp_1$$

$$
\begin{aligned}
&+\wp_7^{\mathrm{T}}\Gamma_0^{\mathrm{T}}M_1+\wp_8^{\mathrm{T}}\Gamma_0^{\mathrm{T}}M_2+X(Ae_2+BFe_3-e_1)\\
&+L_1\mathrm{col}\{e_5,e_7\}+L_2\mathrm{col}\{e_6,e_8\}\big\}+\sigma_0e_3^{\mathrm{T}}\mathscr{Q}e_3, \qquad (28)\\
\Omega_1=&\mathrm{He}\big\{\wp_3^{\mathrm{T}}\mathcal{I}_1^{\mathrm{T}}S_1\wp_2+\wp_4^{\mathrm{T}}\mathcal{I}_1^{\mathrm{T}}S_1\wp_1-L_2\mathrm{col}\{e_{10},e_{12}\}\big\}\\
&+[e_3^{\mathrm{T}}\ e_4^{\mathrm{T}}]S_3[e_3^{\mathrm{T}}\ e_4^{\mathrm{T}}]^{\mathrm{T}}-(e_2-e_3)^{\mathrm{T}}\mathscr{Q}(e_2-e_3)+e_1^{\mathrm{T}}R_1e_1, \qquad (29)\\
\Omega_2=&\mathrm{He}\big\{\wp_5^{\mathrm{T}}\mathcal{I}_2^{\mathrm{T}}S_1\wp_2+\wp_6^{\mathrm{T}}\mathcal{I}_2^{\mathrm{T}}S_1\wp_1-L_1\mathrm{col}\{e_9,e_{11}\}\big\}\\
&-[e_3^{\mathrm{T}}\ e_4^{\mathrm{T}}]S_3[e_3^{\mathrm{T}}\ e_4^{\mathrm{T}}]^{\mathrm{T}}+e_1^{\mathrm{T}}R_2e_1 \qquad (30)
\end{aligned}
$$

with $\mathcal{I}_1=[I\ 0]^{\mathrm{T}}$, $\mathcal{I}_2=[0\ I]^{\mathrm{T}}$ and

$$
\begin{aligned}
&\wp_1=\mathrm{col}\{e_2,e_3,e_4,e_5,e_6,e_7,e_8\},\\
&\wp_2=\mathrm{col}\{e_1,0,0,e_2,-e_2,e_9-e_{11},e_{12}-e_2\},\\
&\wp_3=\mathrm{col}\{e_2-e_3,e_5,e_7\},\ \ \wp_4=\mathrm{col}\{e_1,e_2,e_9-e_{11}\},\\
&\wp_5=\mathrm{col}\{e_4-e_2,e_6,e_8\},\ \ \wp_6=\mathrm{col}\{-e_1,-e_2,e_{12}-e_2\},\\
&\wp_7=\mathrm{col}\{e_2,e_3,e_9,e_{11}\},\ \ \wp_8=\mathrm{col}\{e_4,e_2,e_{10},e_{12}\}.
\end{aligned}
$$

Proof. First, note that

$$
\begin{aligned}
&\varsigma_1(t)=\wp_1\xi(t),\ \dot{\varsigma}_1(t)=\wp_2\xi(t),\ \varsigma_2(t)=\wp_3\xi(t),\\
&\dot{\varsigma}_2(t)=\wp_4\xi(t),\ \varsigma_3(t)=\wp_5\xi(t),\ \dot{\varsigma}_3(t)=\wp_6\xi(t),\\
&\chi_1(t)=\wp_7\xi(t),\ \chi_2(t)=\wp_8\xi(t).
\end{aligned}
$$

Then taking the derivative of $\mathcal{V}_i(t)$ $(i=1,2,3,4)$ yields

$$
\begin{aligned}
\dot{\mathcal{V}}_1(t)=&2\xi^{\mathrm{T}}(t)\Big[\wp_3^{\mathrm{T}}S_2\wp_6+\wp_4^{\mathrm{T}}S_2\wp_5-\wp_3^{\mathrm{T}}\mathcal{I}_1^{\mathrm{T}}S_1\wp_1+\wp_5^{\mathrm{T}}\mathcal{I}_2^{\mathrm{T}}S_1\wp_1\\
&+(s_{k+1}-t)(\wp_3^{\mathrm{T}}\mathcal{I}_1^{\mathrm{T}}S_1\wp_2+\wp_4^{\mathrm{T}}\mathcal{I}_1^{\mathrm{T}}S_1\wp_1)\\
&+(t-s_k)(\wp_5^{\mathrm{T}}\mathcal{I}_2^{\mathrm{T}}S_1\wp_2+\wp_6^{\mathrm{T}}\mathcal{I}_2^{\mathrm{T}}S_1\wp_1)\Big]\xi(t), \qquad (31)\\
\dot{\mathcal{V}}_2(t)=&\xi^{\mathrm{T}}(t)\Big\{(s_{k+1}-t)[e_3^{\mathrm{T}}\ e_4^{\mathrm{T}}]S_3[e_3^{\mathrm{T}}\ e_4^{\mathrm{T}}]^{\mathrm{T}}-(t-s_k)[e_3^{\mathrm{T}}\ e_4^{\mathrm{T}}]S_3[e_3^{\mathrm{T}}\ e_4^{\mathrm{T}}]^{\mathrm{T}}\Big\}\xi(t), \qquad (32)\\
\dot{\mathcal{V}}_3(t)=&(s_{k+1}-t)\dot{x}^{\mathrm{T}}(t)R_1\dot{x}(t)-\int_{s_k}^{t}\dot{x}^{\mathrm{T}}(v)R_1\dot{x}(v)\mathrm{d}v\\
&+(t-s_k)\dot{x}^{\mathrm{T}}(t)R_2\dot{x}(t)-\int_{t}^{s_{k+1}}\dot{x}^{\mathrm{T}}(v)R_2\dot{x}(v)\mathrm{d}v,\\
\dot{\mathcal{V}}_4(t)=&\int_{s_k}^{t}e^{\mathrm{T}}(v)\mathscr{Q}e(v)\mathrm{d}v-(s_{k+1}-t)e^{\mathrm{T}}(t)\mathscr{Q}e(t).
\end{aligned}
$$

For the integral terms in $\dot{\mathcal{V}}_3(t)$, employ Lemma 1 to get

$$
\begin{aligned}
&-\int_{s_k}^{t}\dot{x}^{\mathrm{T}}(v)R_1\dot{x}(v)\mathrm{d}v-\int_{t}^{s_{k+1}}\dot{x}^{\mathrm{T}}(v)R_2\dot{x}(v)\mathrm{d}v\\
&\leqslant-\xi^{\mathrm{T}}(t)\left[\wp_7^{\mathrm{T}}\frac{\Gamma_0^{\mathrm{T}}\mathcal{R}_1\Gamma_0}{t-s_k}\wp_7+\wp_8^{\mathrm{T}}\frac{\Gamma_0^{\mathrm{T}}\mathcal{R}_2\Gamma_0}{s_{k+1}-t}\wp_8\right]\xi(t)\\
&\leqslant\xi^{\mathrm{T}}(t)[(s_{k+1}-t)M_2^{\mathrm{T}}\mathcal{R}_2^{-1}M_2+(t-s_k)M_1^{\mathrm{T}}\mathcal{R}_1^{-1}M_1)]\xi(t)\\
&\quad+\xi^{\mathrm{T}}(t)(2\wp_7^{\mathrm{T}}\Gamma_0^{\mathrm{T}}M_1+2\wp_8^{\mathrm{T}}\Gamma_0^{\mathrm{T}}M_2)\xi(t).
\end{aligned}
$$

The last symbol '$\leqslant$' is obtained using the affine version of Lemma 1. Then

$$
\begin{aligned}
\dot{\mathcal{V}}_3(t)\leqslant&\xi^{\mathrm{T}}(t)\Big[(s_{k+1}-t)(e_1^{\mathrm{T}}R_1e_1+M_2^{\mathrm{T}}\mathcal{R}_2^{-1}M_2)\\
&+(t-s_k)(e_1^{\mathrm{T}}R_2e_1+M_1^{\mathrm{T}}\mathcal{R}_1^{-1}M_1)\\
&+2\wp_7^{\mathrm{T}}\Gamma_0^{\mathrm{T}}M_1+2\wp_8^{\mathrm{T}}\Gamma_0^{\mathrm{T}}M_2\Big]\xi(t). \qquad (33)
\end{aligned}
$$

From the ESS (4), for $t \in [s_k, s_{k+1})$, one has

$$\int_{s_k}^{t} e^{\mathrm{T}}(v)\mathscr{Q}e(v)\mathrm{d}v \leqslant \sigma_0 x^{\mathrm{T}}(s_k)\mathscr{Q}x(s_k). \tag{34}$$

Thus,

$$\begin{aligned}\dot{\mathcal{V}}_4(t) &\leqslant \sigma_0 x^{\mathrm{T}}(s_k)\mathscr{Q}x(s_k) - (s_{k+1}-t)e^{\mathrm{T}}(t)\mathscr{Q}e(t)\\ &= \xi^{\mathrm{T}}(t)[\sigma_0 e_3^{\mathrm{T}}\mathscr{Q}e_3 - (s_{k+1}-t)(e_2-e_3)^{\mathrm{T}}\mathscr{Q}(e_2-e_3)]\xi(t).\end{aligned} \tag{35}$$

On the other hand, it is clear that

$$\begin{bmatrix}\theta_3(t)\\ \theta_7(t)\end{bmatrix} = (t-s_k)\begin{bmatrix}\theta_1(t)\\ \theta_5(t)\end{bmatrix},\ \ \begin{bmatrix}\theta_4(t)\\ \theta_8(t)\end{bmatrix} = (s_{k+1}-t)\begin{bmatrix}\theta_2(t)\\ \theta_6(t)\end{bmatrix},$$

which leads to, for $L_i \in \mathbb{R}^{12n\times 2n}$ $(i=1,2)$

$$2\xi^{\mathrm{T}}(t)L_1\left[\mathrm{col}\{e_5,e_7\} - (t-s_k)\mathrm{col}\{e_9,e_{11}\}\right]\xi(t) = 0, \tag{36}$$

$$2\xi^{\mathrm{T}}(t)L_2\left[\mathrm{col}\{e_6,e_8\} - (s_{k+1}-t)\mathrm{col}\{e_{10},e_{12}\}\right]\xi(t) = 0. \tag{37}$$

From the system (3), for $X \in \mathbb{R}^{12n\times n}$, the following holds:

$$2\xi^{\mathrm{T}}(t)X[(-e_1 + Ae_2 + BFe_3)\xi(t) + Cg(x,t)] = 0. \tag{38}$$

Due to $g(t,x) \in \mathcal{S}_\rho$, for a nonnegative real number $\lambda \geqslant 0$, one has

$$0 \leqslant \lambda\rho^2\xi^{\mathrm{T}}(t)e_2^{\mathrm{T}}\Lambda^{\mathrm{T}}\Lambda e_2\xi(t) - \lambda g^{\mathrm{T}}(t,x)g(t,x). \tag{39}$$

To sum up from (31)–(33) and (35)–(39), together with (24), the estimation on the derivative of $V(t)$ can be given by

$$\begin{aligned}\dot{V}(t) \leqslant& \xi^{\mathrm{T}}(t)\left[\beth_0 + (s_{k+1}-t)\beth_1 + (t-s_k)\beth_2\right]\xi(t)\\ &+ 2\xi^{\mathrm{T}}(t)XCg(x,t) - \lambda g^{\mathrm{T}}(t,x)g(t,x)\\ =& \frac{s_{k+1}-t}{\ell_k}\begin{bmatrix}\xi(t)\\ g(t,x)\end{bmatrix}^{\mathrm{T}}\begin{bmatrix}\beth_0+\ell_k\beth_1 & XC\\ C^{\mathrm{T}}X^{\mathrm{T}} & -\lambda I\end{bmatrix}\begin{bmatrix}\xi(t)\\ g(t,x)\end{bmatrix}\\ &+ \frac{t-s_k}{\ell_k}\begin{bmatrix}\xi(t)\\ g(t,x)\end{bmatrix}^{\mathrm{T}}\begin{bmatrix}\beth_0+\ell_k\beth_2 & XC\\ C^{\mathrm{T}}X^{\mathrm{T}} & -\lambda I\end{bmatrix}\begin{bmatrix}\xi(t)\\ g(t,x)\end{bmatrix},\end{aligned} \tag{40}$$

where $\beth_0 = \Omega_0 + \lambda\rho^2 e_2^{\mathrm{T}}\Lambda^{\mathrm{T}}\Lambda e_2$ and

$$\beth_1 = \Omega_1 + M_2^{\mathrm{T}}\mathcal{R}_2^{-1}M_2,\ \ \beth_2 = \Omega_2 + M_1^{\mathrm{T}}\mathcal{R}_1^{-1}M_1.$$

By the Schur complement, if the matrix inequalities (26) and (27) are satisfied, then

$$\begin{bmatrix}\beth_0+\ell_k\beth_1 & XC\\ C^{\mathrm{T}}X^{\mathrm{T}} & -\lambda I\end{bmatrix} < 0,\ \ \begin{bmatrix}\beth_0+\ell_k\beth_2 & XC\\ C^{\mathrm{T}}X^{\mathrm{T}} & -\lambda I\end{bmatrix} < 0, \tag{41}$$

which lead to $\dot{V}(t) < 0$ for $\ell_k \in [\ell_n, \ell_M]$. Therefore, applying [30, Theorem 1], we can conclude that the system (3) is asymptotically stable for $\forall g(t,x) \in \mathcal{S}_\rho$.

Remark 3. Proposition 1 presents a robust stability criterion for the system (3) with $g(t,x) \in \mathcal{S}_\rho$ under the event-triggered sampling scheme ESS1. One of novelties of Proposition 1 is the introduction of the looped functional $\mathcal{V}_4(t)$, which establishes a seamless connection between the event-triggered sampling scheme ESS1 and the system stability analysis. Moreover, Proposition 1 depends closely on the parameters σ_0, ℓ_m, ℓ_M and ρ. Given a control gain F, the maximum allowable bound ℓ_M can be determined for fixed values of σ_0, ℓ_m and ρ. Similarly, the maximum bound for ρ can be obtained for fixed values of σ_0, ℓ_m and ℓ_M.

5 Control design

In this section, we devise an algorithm to design both the control gain F and the weighted matrix $\mathscr{Q}$ involved in the ESS1, based on Proposition 1. Note that from Proposition 1 the control gain F is only coupled with the matrix X. Thus, we employ a parameter tuning approach for this purpose.

In Proposition 1, we introduce two tuning parameters $\varepsilon_1, \varepsilon_2 \in \mathbb{R}$ such that

$$X = (e_1 + \varepsilon_1 e_2 + \varepsilon_2 e_3)^{\mathrm{T}} \bar{X}^{\mathrm{T}}, \tag{42}$$

where $\bar{X} \in \mathbb{R}^{n\times n}$. Then we can prove that the matrix $\bar{X}$ is nonsingular if the matrix inequalities $\Upsilon_1 < 0$ in (26) and $\Upsilon_2 < 0$ in (27) are satisfied. In fact, note that $e_1(\Omega_0 + \ell_k\Omega_1)e_1^{\mathrm{T}} = -\bar{X} - \bar{X}^{\mathrm{T}} + \ell_k R_1$. If $\Upsilon_1 < 0$ holds, then $\Omega_0 + \ell_k\Omega_1 < 0$, leading to $-\bar{X} - \bar{X}^{\mathrm{T}} + \ell_k R_1 < 0$. Hence, the matrix $\bar{X}$ is invertible. This observation immediately yields the following result.

Proposition 2. For given scalars ρ, ℓ_m, ℓ_M with $\rho \geqslant 0$ and $\ell_M \geqslant \ell_m > 0$, a threshold $\sigma_0 > 0$ and $\varepsilon_1, \varepsilon_2$, the system (1) is asymptotically stabilizable for $\forall g(t,x) \in \mathcal{S}_\rho$ under the event-triggered controller (2) with $F = Y\tilde{X}^{-1}$ if there exist real matrices $\tilde{P} > 0, \tilde{R}_1 > 0, \tilde{R}_2 > 0, \tilde{\mathscr{Q}} > 0$, real matrices $\tilde{S}_1, \tilde{S}_2, \tilde{S}_3, \tilde{M}_1, \tilde{M}_2, \tilde{L}_1, \tilde{L}_2, \tilde{X}, Y$, and a scalar variable $\tilde{\lambda} > 0$ such that, for $\ell_k \in \{\ell_m, \ell_M\}$

$$\tilde{\Upsilon}_1 := \begin{bmatrix} \tilde{\Omega}_0 + \ell_k\tilde{\Omega}_1 & \tilde{\lambda}\wp_0^{\mathrm{T}}C & \rho e_2^{\mathrm{T}}\tilde{X}^{\mathrm{T}}\Lambda^{\mathrm{T}} & \ell_k\tilde{M}_2^{\mathrm{T}} \\ \star & -\tilde{\lambda}I & 0 & 0 \\ \star & \star & -\tilde{\lambda}I & 0 \\ \star & \star & \star & -\ell_k\tilde{\mathcal{R}}_2 \end{bmatrix} < 0, \tag{43}$$

$$\tilde{\Upsilon}_2 := \begin{bmatrix} \tilde{\Omega}_0 + \ell_k\tilde{\Omega}_2 & \tilde{\lambda}\wp_0^{\mathrm{T}}C & \rho e_2^{\mathrm{T}}\tilde{X}^{\mathrm{T}}\Lambda^{\mathrm{T}} & \ell_k\tilde{M}_1^{\mathrm{T}} \\ \star & -\tilde{\lambda}I & 0 & 0 \\ \star & \star & -\tilde{\lambda}I & 0 \\ \star & \star & \star & -\ell_k\tilde{\mathcal{R}}_1 \end{bmatrix} < 0, \tag{44}$$

where $\wp_0 = e_1 + \varepsilon_1 e_2 + \varepsilon_2 e_3$, $\tilde{\mathcal{R}}_i = \mathrm{diag}\{\tilde{R}_i, 3\tilde{R}_i, 5\tilde{R}_i\}$ and

$$\begin{aligned}
\tilde{\Omega}_0 = \mathrm{He}\big\{ & e_2^{\mathrm{T}}\tilde{P}e_1 + \wp_3^{\mathrm{T}}\tilde{S}_2\wp_6 + \wp_4^{\mathrm{T}}\tilde{S}_2\wp_5 + (\wp_5^{\mathrm{T}}\mathcal{I}_2^{\mathrm{T}} - \wp_3^{\mathrm{T}}\mathcal{I}_1^{\mathrm{T}})\tilde{S}_1\wp_1 \\
& + \wp_7^{\mathrm{T}}\Gamma_0^{\mathrm{T}}\tilde{M}_1 + \wp_8^{\mathrm{T}}\Gamma_0^{\mathrm{T}}\tilde{M}_2 + \wp_0^{\mathrm{T}}(A\tilde{X}e_2 + BYe_3 - \tilde{X}e_1) \\
& + \tilde{L}_1\mathrm{col}\{e_5, e_7\} + \tilde{L}_2\mathrm{col}\{e_6, e_8\}\big\} + \sigma_0 e_3^{\mathrm{T}}\tilde{\mathscr{Q}}e_3, \\
\tilde{\Omega}_1 = \mathrm{He}\big\{ & \wp_3^{\mathrm{T}}\mathcal{I}_1^{\mathrm{T}}\tilde{S}_1\wp_2 + \wp_4^{\mathrm{T}}\mathcal{I}_1^{\mathrm{T}}\tilde{S}_1\wp_1 - \tilde{L}_2\mathrm{col}\{e_{10}, e_{12}\}\big\} \\
& + [e_3^{\mathrm{T}}\ e_4^{\mathrm{T}}]\tilde{S}_3[e_3^{\mathrm{T}}\ e_4^{\mathrm{T}}]^{\mathrm{T}} - (e_2 - e_3)^{\mathrm{T}}\tilde{\mathscr{Q}}(e_2 - e_3) + e_1^{\mathrm{T}}\tilde{R}_1 e_1, \\
\tilde{\Omega}_2 = \mathrm{He}\big\{ & \wp_5^{\mathrm{T}}\mathcal{I}_2^{\mathrm{T}}\tilde{S}_1\wp_2 + \wp_6^{\mathrm{T}}\mathcal{I}_2^{\mathrm{T}}\tilde{S}_1\wp_1 - \tilde{L}_1\mathrm{col}\{e_9, e_{11}\}\big\} \\
& - [e_3^{\mathrm{T}}\ e_4^{\mathrm{T}}]\tilde{S}_3[e_3^{\mathrm{T}}\ e_4^{\mathrm{T}}]^{\mathrm{T}} + e_1^{\mathrm{T}}\tilde{R}_2 e_1,
\end{aligned}$$

and the other notations are the same as that in Proposition 1.

Proof. For the specific matrix X given in (42), we define a congruent transformation matrix $\mathcal{T} = \mathrm{diag}\{\mathcal{T}_1, I, I, \mathcal{T}_2\}$ with

$$\mathcal{T}_1 = \textstyle\sum_{i=1}^{12} e_i^{\mathrm{T}}\bar{X}^{-1}e_i,\ \mathcal{T}_2 = \mathrm{diag}\{\bar{X}^{-1}, \bar{X}^{-1}, \bar{X}^{-1}\}.$$

Let

$$\begin{aligned}
& \mathcal{T}_3^{\mathrm{T}}\mathrm{diag}\{P, \mathscr{Q}\}\mathcal{T}_3 = \mathrm{diag}\{\tilde{P}, \tilde{\mathscr{Q}}\},\ \mathcal{T}_3 = \mathrm{diag}\{\bar{X}^{-1}, \bar{X}^{-1}\}, \\
& (\mathrm{diag}\{\mathcal{T}_2, \mathcal{T}_2\})^{\mathrm{T}}S_1\mathrm{diag}\{\mathcal{T}_2, \mathcal{T}_3, \mathcal{T}_3\} = \tilde{S}_1,\ \mathcal{T}_2^{\mathrm{T}}S_2\mathcal{T}_2 = \tilde{S}_2, \\
& \mathcal{T}_3^{\mathrm{T}}S_3\mathcal{T}_3 = \tilde{S}_3,\ \mathcal{T}_3^{\mathrm{T}}\mathrm{diag}\{R_1, R_2\}\mathcal{T}_3 = \mathrm{diag}\{\tilde{R}_1, \tilde{R}_2\}, \\
& \mathcal{T}_1^{\mathrm{T}}M_i\mathcal{T}_2 = \tilde{M}_i,\ \mathcal{T}_1^{\mathrm{T}}L_i\mathcal{T}_3 = \tilde{L}_i,\ (i = 1, 2), \\
& \bar{X}^{-1} = \tilde{X}, \lambda^{-1} = \tilde{\lambda},\ Y = F\tilde{X}.
\end{aligned}$$

Then it is not difficult to verify that

$$\mathcal{T}^{\mathrm{T}}\Upsilon_i\mathcal{T}<0 \iff \tilde{\Upsilon}_i<0\ (i=1,2),$$

where $\tilde{\Upsilon}_1$ and $\tilde{\Upsilon}_2$ are defined in (43) and (44), respectively. The proof is thus completed.

Remark 4. Proposition 2 provides an algorithm to design a suitable event-triggered control gain $F=Y\tilde{X}^{-1}$, together with the weighted matrix $\mathscr{Q}=\tilde{X}^{-T}\tilde{\mathscr{Q}}\tilde{X}^{-1}$. This algorithm is linearly dependent on the upper bound ℓ_M of sampling intervals ℓ_k's and the upper bound ρ related to the set $\mathcal{S}_\rho$. For a given ℓ_M, the local optimal value $\rho_{\max}$ can be derived from Proposition 2 by tuning two parameters ε_1 and ε_2. A numerical optimization algorithm, such as fminsearch in the optimization toolbox, can be used to find an optimal combination of these tuning parameters ε_1 and ε_2.

With Proposition 2, an implementation of the ESS1 is given in Algorithm 1. From this algorithm, one can see clearly that the ESS1 works well even if the system under study is approaching its steady state.

Algorithm 1 Implementation of the ESS1.

Input: System matrices A,B,C and Λ and a threshold σ_0 and the lower bound ℓ_m.

Step 1. Find the local optimal values of ℓ_M and ρ by solving the following optimization problems OP1 for fixed ρ and OP2 for fixed ℓ_M:

$$\text{OP1:}\quad \max_{\varepsilon_1,\varepsilon_2\in\mathbb{R}}\ell_M \qquad \text{subject to}\ \ (43),(44), \tag{45}$$

$$\text{OP2:}\quad \max_{\varepsilon_1,\varepsilon_2\in\mathbb{R}}\rho \qquad \text{subject to}\ \ (43),(44). \tag{46}$$

Step 2. Co-design the weighted matrix $\mathscr{Q}$ in the ESS1 and the control gain F using Proposition 2 with the local optimal values of ρ and ℓ_M from Step 1.

Step 3. Trigger the next event at $t=s_{k+1}$

$$s_{k+1}=\min\Big\{s_k+\ell_M,\inf\big\{t>s_k|\mathscr{T}(t)>0\big\}\Big\}. \tag{47}$$

6 Numerical examples

In this section, we verify the advantages of the proposed results over some existing ones through two practical systems.

Example 1. Consider the batch reactor model [37] with its state space description given as (1) with $C=0$ and

$$A=\begin{bmatrix}1.38 & -0.2 & 6.71 & -5.67\\ -0.58 & -4.29 & 0 & 0.67\\ 1.06 & 4.27 & -6.65 & 5.89\\ 0.04 & 4.27 & 1.34 & -2.1\end{bmatrix},\quad B=\begin{bmatrix}0 & 0\\ 5.67 & 0\\ 1.13 & -3.14\\ 1.13 & 0\end{bmatrix}.$$

From [38], the controller $u(t)=Fx(t)$ can stabilize the system, where

$$F=\begin{bmatrix}0.1006 & -0.2469 & -0.0952 & -0.2447\\ 1.4099 & -0.1966 & 0.0139 & 0.0823\end{bmatrix}.$$

The initial state is set as $x_0=\mathrm{col}\big\{6\sin(0.5),6\cos(0.5),1,9\big\}$.

We present this example to demonstrate the effectiveness of the proposed event-triggered sampling scheme ESS1. To this end, we compare it with event-triggered schemes using the conditions $\mathscr{T}_i(t)>0$ defined in (17)–(19).

Let $\mathscr{Q}=I$ and $\sigma_0=0.1$. The system responses and sampling intervals are plotted in Figures 1–4, respectively, under the event-triggered sampling schemes with $\mathscr{T}_1(t)$, $\mathscr{T}_2(t)$, $\mathscr{T}_3(t)$, and ESS1. The corresponding number of triggered events is 108, 74, 61, and 40, respectively.

From these figures, it can be observed that under ESS1, the system reaches its steady state almost simultaneously with the event-triggered schemes using $\mathscr{T}_1(t)>0$ and $\mathscr{T}_2(t)>0$, while the number of events triggered is significantly lower compared to event-triggered schemes using $\mathscr{T}_1(t)>0$ and $\mathscr{T}_2(t)>0$. Although the event-triggered scheme with $\mathscr{T}_3(t)$ triggers fewer events during the time period $[0,30]$ s, the system requires much more time to reach its steady state.

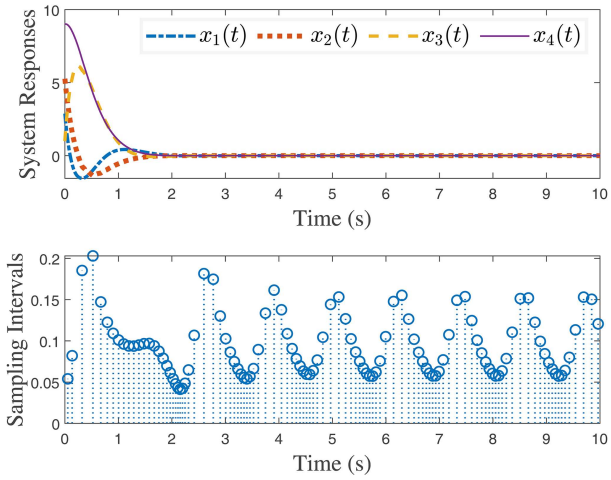

Figure 1 (Color online) State responses and time-intervals from the event-triggered scheme with $\mathscr{T}_1(t)$ in (17) for Example 1.

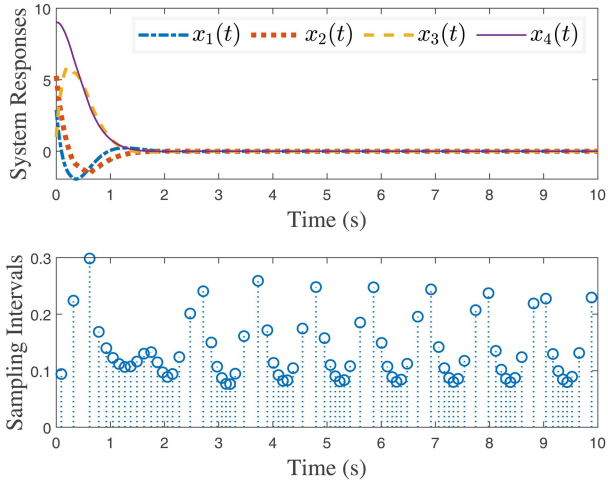

Figure 2 (Color online) State responses and time-intervals from the event-triggered scheme with $\mathscr{T}_2(t)$ in (18) for Example 1.

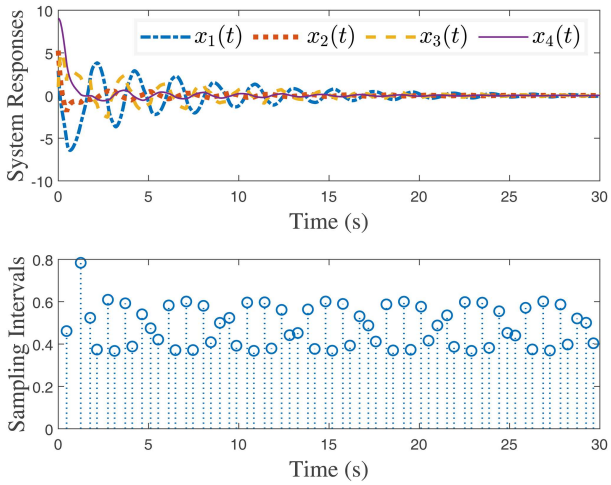

Figure 3 (Color online) State responses and time-intervals from the event-triggered scheme with $\mathscr{T}_3(t)$ in (19) for Example 1.

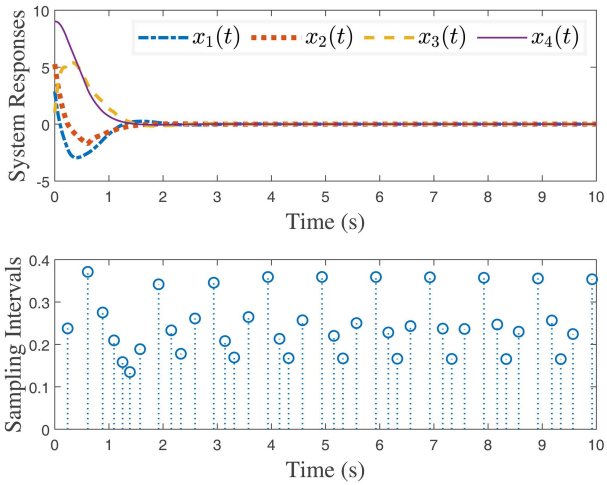

Figure 4 (Color online) State responses and time-intervals from the event-triggered scheme ESS1 for Example 1.

Example 2. Consider a practical system comprising two identical pendulums that are coupled by a spring, as depicted in Figure 5 [31]. Its equations of motion are given as

$$ml^2\ddot{\theta}_1 = mgl\theta_1 - ka^2(\theta_1 - \theta_2) + u_1,$$
$$ml^2\ddot{\theta}_2 = mgl\theta_2 - ka^2(\theta_2 - \theta_1) + u_2.$$

Set $x = \mathrm{col}\{\theta_1, \dot{\theta}_1, \theta_2, \dot{\theta}_2\}$ and $u = \mathrm{col}\{u_1, u_2\}$. Suppose that the spring can move up and down the rods of the pendulums in sudden jumps of unpredictable size and direction, between the support and a height ρ. This implies that the time-varying parameter $a(t,x)$ is a piecewise continuous function in both time and state such that $0 \leqslant a(t,x) \leqslant \rho$. Let $g(t,x) = a(t,x)x$ and set $g/l = 1$, $1/(ml^2) = 1$, and $k/(ml^2) = 1$. Then the dynamic equations of the system can be described as (1), where

$$A = \begin{bmatrix} 0 & 1 & 0 & 0 \\ 1 & 0 & 0 & 0 \\ 0 & 0 & 0 & 1 \\ 0 & 0 & 1 & 0 \end{bmatrix}, \quad B = \begin{bmatrix} 0 & 0 \\ 1 & 0 \\ 0 & 0 \\ 0 & 1 \end{bmatrix}, \quad C = \begin{bmatrix} 0 & 0 & 0 & 0 \\ -1 & 0 & 1 & 0 \\ 0 & 0 & 0 & 0 \\ 1 & 0 & -1 & 0 \end{bmatrix}.$$

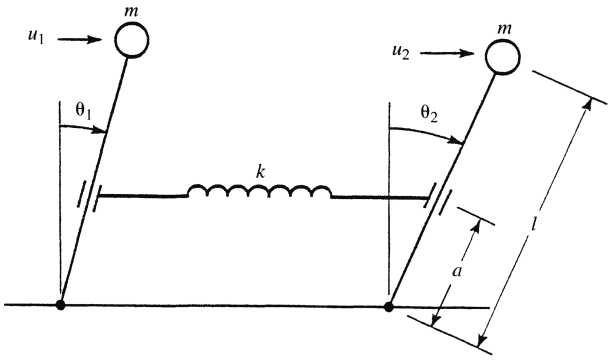

Figure 5 Inverted pendulums.

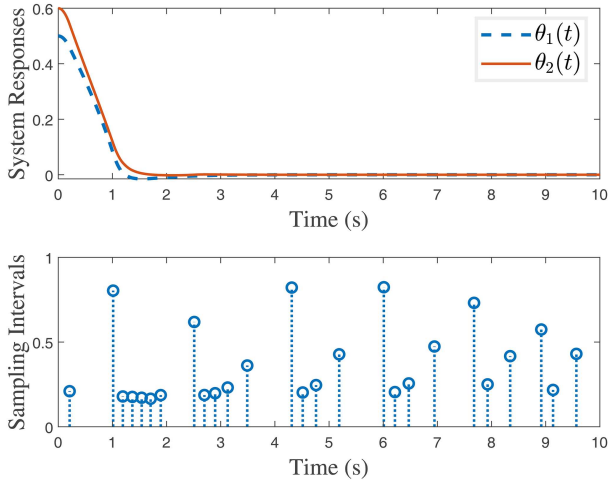

Figure 6 (Color online) State responses for Example 2 under ESS1.

Table 1 The obtained $\rho_{\max}$ of ρ for different ℓ_M ($\ell_m = 10^{-5}$).

	$\ell_M = 0.15$	$\ell_M = 0.2$	$\ell_M = 0.25$	$\ell_M = 0.3$	$\ell_M = 0.35$
$\rho_{\max}$	2.59	2.02	1.63	1.33	1.11

This system is studied in [31]. The aim is to design a suitable state feedback controller such that the resultant closed-loop system is asymptotically stable with ρ being as big as possible. By introducing a decentralized state feedback controller, it is found that the system is stabilizable for $\forall \rho \leqslant \rho_{\max} = 1$.

Now we turn to the event-triggered control scheme ESS1 to consider the problem above. For $\ell_m = 10^{-5}, \ell_M = 0.25$ and $\sigma_0 = 0.2$, applying Proposition 2 with $\varepsilon_1 = 1.5$ and $\varepsilon_2 = 2$, a local optimal value $\rho_{\max}$ of ρ can be obtained as $\rho_{\max} = 1.63$, which is much larger than the one from [31]. Moreover, the corresponding weighted matrix $\mathscr{Q}$ and the control gain F can be co-designed as

$$\mathscr{Q} = \begin{bmatrix} 0.1097 & 0.0904 & 0.1092 & 0.0904 \\ 0.0904 & 0.1142 & 0.0904 & 0.1141 \\ 0.1092 & 0.0904 & 0.1097 & 0.0904 \\ 0.0904 & 0.1141 & 0.0904 & 0.1142 \end{bmatrix},$$

$$F = \begin{bmatrix} -5.0840 & -4.7767 & -0.0169 & 0.3480 \\ -0.0169 & 0.3480 & -5.0840 & -4.7767 \end{bmatrix}.$$

Under the controller obtained above, according to Algorithm 1, the state responses are plotted in Figure 6, where sampling intervals are also given. It is clear that the closed-loop system is asymptotically stable for $\forall \rho \leqslant 1.63$. Moreover, Table 1 lists the maximum $\rho_{\max}$ for different values of ℓ_M obtained by Proposition 2 with $\sigma_0 = 0.2, \varepsilon_1 = 1.5$ and $\varepsilon_2 = 2$. From this table, one can see clearly that, as the sampling intervals ℓ_M grows, the allowable upper bound of ρ decreases.

7 Conclusion

This paper has addressed the problem of event-triggered stabilization for a class of nonlinear networked systems. Based on the integral of the error vector's norm, a novel event-triggered sampling scheme has been proposed. It has been proven that this scheme not only eliminates Zeno behavior but also performs more effectively, especially when the system signal exhibits little fluctuation. Then, a novel looped functional tailored to the proposed event-triggered scheme has been constructed to formulate a sampling-interval-dependent robust stability criterion for the closed-loop system. Utilizing this criterion, an algorithm has been presented for the co-design of control gains and event-triggered parameters. Finally, two examples have been given to demonstrate the effectiveness of the proposed method. In our future research, we will focus on the extension of the proposed ETS to multi-agent systems [39–41]

and direct-drive-wheel systems [42].

Open Access funding enabled and organized by CAUL and its Member Institutions.

References

1 Tabuada P. Event-triggered real-time scheduling of stabilizing control tasks. IEEE Trans Automat Contr, 2007, 52: 1680–1685
2 Aström K. Event Based Control. Berlin: Springer, 2008. 127–147
3 Zhang X M, Han Q L, Ge X, et al. An overview of recent advances in event-triggered control. Sci China Inf Sci, 2025, 68: 161201
4 Peng C, Li F. A survey on recent advances in event-triggered communication and control. Inf Sci, 2018, 457-458: 113–125
5 Li H, Liu Y, Li F. Event-triggered output-feedback stabilization with prescribed convergence rate. IEEE Trans Ind Inf, 2023, 19: 2847–2855
6 Xiao H C, Ding D R, Dong H L, et al. Adaptive event-triggered state estimation for large-scale systems subject to deception attacks. Sci China Inf Sci, 2022, 65: 122207
7 Wang X, Sun J, Deng F, et al. Event-triggered consensus control of heterogeneous multi-agent systems: model- and data-based approaches. Sci China Inf Sci, 2023, 66: 192201
8 Sun Q, Chen J C, Shi Y. Event-triggered robust MPC of nonlinear cyber-physical systems against DoS attacks. Sci China Inf Sci, 2022, 65: 110202
9 Wei Q, Jiao S, Dong Q, et al. Event-triggered robust parallel optimal consensus control for multiagent systems. IEEE CAA J Autom Sin, 2025, 12: 40–53
10 Zhang Z, Shi K, Chen H, et al. An improved integral-based adaptive event-triggered frequency regulation on a dual-link LFC system under mixed attacks. IEEE Trans Syst Man Cybern Syst, 2024, 54: 5160–5171
11 Yuan Y, He W, Du W, et al. Distributed gradient tracking for differentially private multi-agent optimization with a dynamic event-triggered mechanism. IEEE Trans Syst Man Cybern Syst, 2024, 54: 3044–3055
12 Zhang X M, Han Q L, Ge X, et al. Sampled-data control systems with non-uniform sampling: a survey of methods and trends. Annu Rev Control, 2023, 55: 70–91
13 Miskowicz M. Event-based Control and Signal Processing. New York: CRC Press, 2015
14 Lai J, Lu X, Yu X, et al. Stochastic distributed secondary control for AC microgrids via event-triggered communication. IEEE Trans Smart Grid, 2020, 11: 2746–2759
15 Lehmann D, Lunze J. Event-based control with communication delays and packet losses. Int J Control, 2012, 85: 563–577
16 Ding D R, Han Q L, Ge X H, et al. Privacy-preserving filtering, control and optimization for industrial cyber-physical systems. Sci China Inf Sci, 2025, 68: 141201
17 Yang F, Xie X, Sun Q, et al. FDI attack estimation and event-triggered resilient control of DC microgrids under hybrid attacks. IEEE Trans Smart Grid, 2024, 15: 4207–4216
18 Yang H, Peng C, Cao Z, et al. A novel semantic-based multi-packet parallel transmission scheme for networked control systems. Automatica, 2025, 174: 112120
19 Zeng H B, Zhu Z J, Peng T S, et al. Robust tracking control design for a class of nonlinear networked control systems considering bounded package dropouts and external disturbance. IEEE Trans Fuzzy Syst, 2024, 32: 3608–3617
20 Zhang X M, Han Q L, Ge X. A novel approach to H_∞ performance analysis of discrete-time networked systems subject to network-induced delays and malicious packet dropouts. Automatica, 2022, 136: 110010
21 Yu H, Hao F. Input-to-state stability of integral-based event-triggered control for linear plants. Automatica, 2017, 85: 248–255
22 Mousavi S H, Ghodrat M, Marquez H J. Integral-based event-triggered control scheme for a general class of non-linear systems. IET Control Theor Appl, 2015, 9: 1982–1988
23 Rsetam K, Cao Z, Man Z, et al. GPIO-based continuous sliding mode control for networked control systems under communication delays with experiments on servo motors. IEEE CAA J Autom Sin, 2025, 12: 99–113
24 Zhang L, Nguang S K, Ouyang D, et al. Synchronization of delayed neural networks via integral-based event-triggered scheme. IEEE Trans Neural Netw Learn Syst, 2020, 31: 5092–5102
25 Zhang X M, Han Q L, Zhang B L, et al. Accumulated-state-error-based event-triggered sampling scheme and its application to H∞ control of sampled-data systems. Sci China Inf Sci, 2024, 67: 162206
26 Borgers D P, Heemels W P M H. Event-separation properties of event-triggered control systems. IEEE Trans Automat Contr, 2014, 59: 2644–2656
27 Ghodrat M, Marquez H J. A new Lyapunov-based event-triggered control of linear systems. IEEE Trans Automat Contr, 2023, 68: 2599–2606
28 Wang X H, Wang Z, Xia J W, et al. Adaptive event-trigger-based sampled-data stabilization of complex-valued neural networks: a real and complex LMI approach. Sci China Inf Sci, 2023, 66: 149203

29 Girard A. Dynamic triggering mechanisms for event-triggered control. IEEE Trans Automat Contr, 2015, 60: 1992–1997

30 Seuret A. A novel stability analysis of linear systems under asynchronous samplings. Automatica, 2012, 48: 177–182

31 Šiljak D D, Stipanović D M. Robust stabilization of nonlinear systems: the LMI approach. Math Problems Eng, 2000, 6: 461–493

32 Yu M, Wang L, Chu T G. Robust stabilization of nonlinear sampled-data systems. In: Proceedings of the American Control Conference, 2005. 3421–3426

33 Peng C, Tian Y C, Tadé M O. State feedback controller design of networked control systems with interval time-varying delay and nonlinearity. Intl J Robust Nonlinear, 2008, 18: 1285–1301

34 Miskowicz M. Asymptotic effectiveness of the event-based sampling according to the integral criterion. Sensors, 2007, 7: 16–37

35 Zhang X M, Han Q L, Ge X, et al. An overview of recent developments in Lyapunov-Krasovskii functionals and stability criteria for recurrent neural networks with time-varying delays. Neurocomputing, 2018, 313: 392–401

36 Liu K, Fridman E. Wirtinger's inequality and Lyapunov-based sampled-data stabilization. Automatica, 2012, 48: 102–108

37 Walsh G, Ye H. Scheduling of networked control systems. IEEE Control Sys Mag, 2001, 21: 57–65

38 Mazo M, Anta A, Tabuada P. On self-triggered control for linear systems: guarantees and complexity. In: Proceedings of the 10th European Control Conference, 2009. 3767–3772

39 Jia X, Li H, Chi X, et al. Leader-following secure output consensus of heterogeneous multiagent systems based on two sampling mechanisms under hybrid cyber-attacks. IEEE Trans Cybern, 2024, 54: 7826–7838

40 Li B, Jia X, Chi X, et al. Consensus for second-order multiagent systems under two types of sampling mechanisms: a time-varying gain observer method. IEEE Trans Cybern, 2022, 52: 8061–8072

41 Ge X, Han Q L, Zhang X M, et al. Distributed coordination control of multi-agent systems under intermittent sampling and communication: a comprehensive survey. Sci China Inf Sci, 2025, 68: 151201

42 Zhang D, Han Q L, Zhang X M. Network-based modeling and proportional-integral control for direct-drive-wheel systems in wireless network environments. IEEE Trans Cybern, 2020, 50: 2462–2474